Received: 19 June 2016 | Revised: 12 January 2017 | Accepted: 13 January 2017

DOI 10.1002/acs.2761

WILEY

RESEARCH ARTICLE

Adaptive sliding mode–based diagnosis of actuator faults for LPV systems

Sandy Rahme[1] | **Nader Meskin**[1] | **Javad Mohammadpour**[2]

[1]Department of Electrical Engineering, Qatar University, Doha, Qatar
[2]School of Electrical & Computer Engineering, College of Engineering, The University of Georgia, Athens, GA 30602, USA

Correspondence
Nader Meskin, Department of Electrical Engineering, Qatar University, Doha, Qatar.
Email: nader.meskin@qu.edu.qa

Funding information
NPRP, Grant/Award Number: 5-574-2-233; Qatar National Research Fund

Summary

In this paper, an adaptive sliding mode observer is developed for actuator fault diagnosis of linear parameter–varying systems. The main advantage of the proposed approach is its ability to cope with time-varying distribution matrix in linear parameter–varying systems. Furthermore, the proposed adaptive observer is characterized by its output robustness against parameter uncertainties and disturbances without any a priori knowledge about their bounds. The efficiency of the proposed fault diagnosis approach is validated using simulation studies.

KEYWORDS

fault diagnosis, LPV system, Matlab/Simulink, sliding mode observer

1 | INTRODUCTION

Fault detection and isolation (FDI) module is an important unit in industrial systems that provides essential information regarding the occurrence of faults in these systems. With a fast and accurate fault diagnosis algorithm, fault consequences can be alleviated or even eliminated, and fault-tolerant controllers can be reconfigured to maintain a certain level of performance. Fault detection and isolation filters designed on the basis of linear models usually reach the desired performance around a specific operating point. However, the system might encounter a performance degradation as it moves away from the operating point, which leads to false alarms or missing fault detection. The linear parameter–varying (LPV) framework offers a formal way to extend the FDI methodologies based on linear time–invariant (LTI) systems to develop FDI filter design approaches for nonlinear/time-varying systems.[1] For LPV systems, the FDI filter gains are automatically scheduled based on a number of measurable variables called scheduling variables.[2,3] The main feature of LPV-based FDI design is the guaranteed stability and performance over a wide range of operation.[4-6] Moreover, it is worth mentioning that although new nonlinear model-based FDI design approaches have been developed for nonlinear systems,[7] the LPV observer designs have widely used linear design methodologies to be applied to nonlinear systems.

Many techniques have been developed for fault diagnosis of LPV systems in the literature such as the geometric approach,[8] the inversion based methods,[9] the eigenstructure assignment,[10] robust approaches like the norm-based optimization filters,[7,11-13] interval observers,[14] unknown input observers,[15] and sliding mode observers.[16,17] Despite the benefits of LPV-based FDI filter design approaches, the LPV model used as the basis of the LPV observer design might not perfectly represent the original nonlinear behavior of the system, which may eventually lead to false alarms or missing detections. Furthermore, plant-model mismatch, uncertainties, and faulty sensor measurements are other factors that have to be taken into consideration.

Sliding mode design is a powerful tool to adopt for LPV systems because of its high robustness against parametric uncertainties and perturbations. Compared with previous sliding mode observers designed with fixed gain for LPV systems,[16,17] 1 benefit of the adaptive sliding mode approach is that the observer gain is continuously updated to overcome the system uncertainties and faults without any a priori knowledge about their bounds.[18-20] Hence, the obtained gain has a sufficient value leading to stability while reducing the chattering phenomenon. Furthermore, in the literature, the design of sliding mode observer for LPV systems has been restricted to a class of LPV systems with fixed output distribution matrix[16,17,21] that is required for several complicated

algebraic manipulations for the fault reconstruction procedure. In this paper, we consider a time-varying output distribution matrix that depends on scheduling variables; this represents a wide range of nonlinear systems especially in the chemical processes. Therefore, another benefit of the proposed LPV adaptive sliding mode observer is its ability to cope with the time-varying output distribution matrix after ensuring its nonsingularity, boundedness, and its derivative boundedness over all the trajectories of the scheduling variables. Using the proposed technique, we generalize the fault diagnosis for time-varying distribution matrices and can be further used for LPV models with a fixed distribution matrix. Theoretical derivations from Lyapunov stability conditions guarantee the stability and robustness of the adaptive sliding mode observer designed for LPV systems. Finally, the convergence of the sliding mode observer allows to directly detect, isolate, and estimate of the size and severity of the fault by analyzing the so-called equivalent output estimation error injection concept.[22-24]

The paper is organized as follows. In Section 2, some preliminaries are presented for the LPV system analysis. Then, an LPV adaptive sliding mode observer design method is described in Section 3 for the reformulated LPV model. The proposed observer is validated in Section 4 via simulation study using LPV models with fixed and time-varying output distribution matrices. Finally, concluding remarks are made in Section 5.

Notation: In this paper, $\mathbb{R}^n_+$ represents the set of vectors in $\mathbb{R}^n$ with positive elements. $(\cdot)^\top$ denotes the transpose of a vector or matrix, $|\cdot|$ denotes the absolute value, and $||\cdot||$ represents the Euclidean norm or induced norm. Finally, I_p is a $p \times p$ identity matrix.

2 | LINEAR PARAMETER–VARYING SYSTEMS ANALYSIS

Consider an LPV system described by

$$\begin{aligned} \dot{x}(t) &= A(\theta(t))x(t) + B(\theta(t))u(t) + Ew(t) + Hf_a(t), \quad x(0) = x_0, \\ y(t) &= C(\theta(t))x(t), \end{aligned} \tag{1}$$

where the state vector is $x(t) \in \mathbb{R}^n$, $t \geqslant 0$, the input vector is $u(t) \in \mathbb{R}^m$, $t \geqslant 0$, and the output vector is $y(t) \in \mathbb{R}^p$, $t \geqslant 0$. The matrices $A(\theta) \in \mathbb{R}^{n\times n}$, $B(\theta) \in \mathbb{R}^{n\times m}$, and $C(\theta) \in \mathbb{R}^{p\times n}$ are matrix functions dependent on the scheduling variables $\theta(t)$, $t \geqslant 0$, and $E \in \mathbb{R}^{n\times r}$, and $H \in \mathbb{R}^{n\times q}$ are constant matrices. To simplify the notations, θ will be used to denote the time-varying scheduling variables $\theta(t)$. The unknown term $w(t) \in \mathbb{R}^r$, $t \geqslant 0$, represents all modeling uncertainties and disturbances experienced by the system, and the unknown function $f_a(t) \in \mathbb{R}^q$, $t \geqslant 0$, represents the actuator fault with $q \leqslant p < n$.

For more general LPV models where the fault signature matrix $H(\theta)$ is time-varying, $H(\theta)$ can be factorized into $H(\theta) = HF(\theta)$ where $H \in \mathbb{R}^{n\times q}$ is fixed and $F(\theta) \in \mathbb{R}^{q\times q}$ is a parameter-varying matrix assumed to be invertible. By this change of variable, the matrix H will be constant as in Equation 1, and the new fault signal is considered as $f_b(t) = F(\theta)f_a(t)$. The proposed observer design strategy will initially estimate $f_b(t)$, and then $f_a(t)$ will be obtained as $f_a(t) = F^{-1}(\theta)f_b(t)$.

The scheduling variable θ is defined over a compact scheduling set $P_\theta \subset \mathbb{R}^m$ such that $\theta : \mathbb{R} \to \mathbb{P}_\theta$. P_θ considered as a polytope is defined as the convex hull given by the vertices θ_{v_i} such that $P_\theta := \text{Co}\{\theta_{v_1}, \theta_{v_2}, \dots, \theta_{v_M}\}$, where $M = 2^m$, is found by only considering the bounds of θ_i, and $Co\{\cdot\}$ denotes a convex hull. It is also assumed that $\dot{\theta}(t)$ is bounded and that $\dot{\theta}(t) : \mathbb{R} \to \mathbb{P}_{\dot{\theta}}$, where $P_{\dot{\theta}} := \text{Co}\{\dot{\theta}_{v_1}, \dot{\theta}_{v_2}, \dots, \dot{\theta}_{v_M}\}$. The LPV matrices in Equation 1, represented by the matrix $Q(\theta)$ where $Q \in \{A, B, C\}$, are continuous functions that are assumed to depend affinely on θ as

$$Q(\theta) = Q_0 + \sum_{i=1}^{m} \theta_i Q_i, \tag{2}$$

where θ_i is the i^{th} element of θ. Since θ can be expressed as a convex combination of M vertices θ_{v_i}, the system can be represented by a linear combination of LTI models at the vertices. As a result, each matrix in Equation 1 is represented in a polytopic form as

$$Q(\theta) = \sum_{i=1}^{M} \alpha_i Q\left(\theta_{v_i}\right), \tag{3}$$

such that $\sum_{i=1}^{M} \alpha_i = 1$ and $\alpha_i \geqslant 0$. Before designing the fault diagnosis observer, some assumptions will be considered for the system (Equation 1).

Assumption 1. It is assumed that rank $(C(\theta)[EH])$ = rank $([EH]) = \tilde{q} \leqslant p$.

Lemma 1. Under *Assumption*1, there exists a coordinate transformation $x \mapsto \mathcal{T}x$ in which the triple $(A, [EH], C(\theta))$ has the following structure:

$$\left(\begin{bmatrix} A_1(\theta) & A_2(\theta) \\ A_3(\theta) & A_4(\theta) \end{bmatrix}, \begin{bmatrix} 0_{(n-p)\times r} & 0_{(n-p)\times q} \\ E_2 & H_2 \end{bmatrix}, \begin{bmatrix} 0_{p\times(n-p)} & C_2(\theta) \end{bmatrix} \right), \tag{4}$$

where $A_1(\theta) \in \mathbb{R}^{(n-p)\times(n-p)}$, $C_2(\theta) \in \mathbb{R}^{p\times p}$ is nonsingular,

$$E_2 = \begin{bmatrix} 0_{(p-\tilde{q})\times r} \\ E_{22} \end{bmatrix} \text{ and } H_2 = \begin{bmatrix} 0_{(p-\tilde{q})\times q} \\ H_{22} \end{bmatrix}, \tag{5}$$

$E_{22} \in \mathbb{R}^{\tilde{q}\times r}$ and the matrix $H_{22} \in \mathbb{R}^{\tilde{q}\times q}$ is of full rank.

Proof. Following the same reasoning as for LTI systems given in the work of Yan and Edwards[25] and without the loss of generality, the output matrix is assumed to have the following form:

$$C(\theta) = [0 \;\; \tilde{C}_2(\theta)],$$

with $\tilde{C}_2(\theta) \in \mathbb{R}^{p\times p}$ as a full rank matrix, and the partition $[EH]$ is in a compatible way with $C(\theta)$ as

$$[E \;\; H] = \begin{bmatrix} \tilde{E}_1 & \tilde{H}_1 \\ \tilde{E}_2 & \tilde{H}_2 \end{bmatrix}, \tag{6}$$

where $\tilde{E}_1 \in \mathbb{R}^{(n-p)\times r}$ and $\tilde{H}_1 \in \mathbb{R}^{(n-p)\times q}$. It follows that rank $(C(\theta)[EH])$ = rank $(\tilde{C}_2(\theta)[\tilde{E}_2 \;\; \tilde{H}_2])$.

Since $\tilde{C}_2(\theta) \in \mathbb{R}^{p\times p}$ is of full rank, one can conclude that rank $(\tilde{C}_2(\theta)[\tilde{E}_2 \;\; \tilde{H}_2])$=rank $([\tilde{E}_2 \;\; \tilde{H}_2])$.

Furthermore, from Assumption 1, rank $([\tilde{E}_2 \;\; \tilde{H}_2])$=$([EH])$, which implies that there exists a matrix $\tilde{V} \in \mathbb{R}^{(n-p)\times p}$ such that

$$[\tilde{E}_1 \;\; \tilde{H}_1] = \tilde{V}[\tilde{E}_2 \;\; \tilde{H}_2] = [\tilde{V}\tilde{E}_2 \;\; \tilde{V}\tilde{H}_2].$$

Moreover, rank $([\tilde{E}_2 \;\; \tilde{H}_2])$= $\tilde{q}$ implies that there exists a nonsingular matrix $\tilde{T} \in \mathbb{R}^{p\times p}$ such that

$$\tilde{T}[\tilde{E}_2 \;\; \tilde{H}_2] = \begin{bmatrix} 0_{(p-\tilde{q})\times r} & 0_{(p-\tilde{q})\times q} \\ E_{22} & H_{22} \end{bmatrix} = [E_2 \;\; H_2]. \tag{7}$$

If the nonsingular matrix $\mathcal{T} \in \mathbb{R}^{n\times n}$ is constructed as

$$\mathcal{T} = \begin{bmatrix} I_{n-p} & -\tilde{V} \\ 0 & \tilde{T} \end{bmatrix},$$

then it follows from Equations 6 and 7 that

$$\mathcal{T}[E \;\; H] = \begin{bmatrix} 0_{(n-p)\times r} & 0_{(n-p)\times q} \\ 0_{(p-\tilde{q})\times r} & 0_{(p-\tilde{q})\times q} \\ E_{22} & H_{22} \end{bmatrix}, \tag{8}$$

$$C\mathcal{T}^{-1} = [0_{p\times(n-p)} \;\; \tilde{C}_2(\theta)\tilde{T}^{-1}]. \tag{9}$$

Letting $C_2(\theta) = \tilde{C}_2(\theta)\tilde{T}^{-1}$ leads to the same structures of the matrices as given in Equations 4 and 5. □

From Lemma 1, the system (Equation 1) can be rewritten in the following form

$$\begin{aligned} \dot{x}_1(t) &= A_1(\theta)x_1(t) + A_2(\theta)x_2(t) + B_1(\theta)u(t), \\ \dot{x}_2(t) &= A_3(\theta)x_1(t) + A_4(\theta)x_2(t) + B_2(\theta)u(t) + E_2w(t) + H_2f_a(t), \\ y(t) &= C_2(\theta)x_2(t), \end{aligned} \tag{10}$$

where $x_1(t) \in \mathbb{R}^{n-p}$, $t \geqslant 0$, and the matrices are as defined in Lemma 1. Let us introduce the following transformation

$$T = \begin{bmatrix} I_{n-p} & L \\ 0 & I_p \end{bmatrix}, \tag{11}$$

where L has the following structure

$$L = [L_1 \; 0_{(n-p)\times\tilde{q}}] \in \mathbb{R}^{(n-p)\times p}, \tag{12}$$

with $L_1 \in \mathbb{R}^{(n-p)\times(p-\tilde{q})}$ to be designed later on. Then, it follows that the system (Equation 10) has the following representation in the new coordinate system $z = Tx$:

$$\begin{aligned} \dot{z}_1(t) &= (A_1(\theta) + LA_3(\theta))\, z_1(t) + (A_2(\theta) + LA_4(\theta) \\ &\quad - (A_1(\theta) + LA_3(\theta))\, L)\, z_2(t) \\ &\quad + (B_1(\theta) + LB_2(\theta))\, u(t), \\ \dot{z}_2(t) &= A_3(\theta)z_1(t) + (A_4(\theta) - A_3(\theta)L)\, z_2(t) + B_2(\theta)u(t) \\ &\quad + E_2w(t) + H_2f_a(t), \\ y(t) &= C_2(\theta)z_2(t). \end{aligned} \tag{13}$$

After analyzing and reformulating the problem for LPV systems, the design of an LPV adaptive sliding mode observer is addressed in the next section.

3 | ADAPTIVE SLIDING MODE OBSERVER DESIGN FOR LPV SYSTEMS

The sliding mode observer consists of a discontinuous signal $\nu(t)$ designed to drive the system to reach the desired sliding surface $\sigma(y, \hat{y}, t) = \hat{y}(t) - y(t) = 0$, with $\hat{y}(t)$ being the observer output, and to maintain the sliding motion around it.[22] For the actuator fault diagnosis, an LPV adaptive sliding mode observer is designed here inspired by the LTI sliding mode strategy proposed in previous studies.[19,20] With the adaptive sliding mode approach, no a priori knowledge of the uncertainty and perturbation bounds is required. The observer gain will be increasing until the sliding motion starts around $\sigma(y, \hat{y}, t) = 0$. The gain will keep its value after reaching the sliding surface. Consequently, the induced chattering is reduced because of the gain of the discontinuous signal $\nu(t)$ is not overestimated.

The sliding mode observer to be designed is described by

$$\begin{aligned} \dot{\hat{z}}_1(t) &= (A_1(\theta) + LA_3(\theta))\, \hat{z}_1(t) + (A_2(\theta) + LA_4(\theta) \\ &\quad - (A_1(\theta) + LA_3(\theta))\, L)\, C_2^{-1}(\theta)y(t) \\ &\quad + (B_1(\theta) + LB_2(\theta))\, u(t), \\ \dot{\hat{z}}_2(t) &= A_3(\theta)\hat{z}_1(t) + (A_4(\theta) - A_3(\theta)L)\, \hat{z}_2(t) + B_2(\theta)u(t) \\ &\quad - K\,(\hat{y}(t) - y(t)) + C_2^{-1}(\theta)\nu(t), \\ \hat{y}(t) &= C_2(\theta)\hat{z}_2(t), \end{aligned} \tag{14}$$

where the observer gain $K \in \mathbb{R}^{p\times p}$ and $L \in \mathbb{R}^{(n-p)\times p}$ of the form (Equation 12) are introduced to guarantee the stability of the observer error system. The j^{th} component $\nu_j(t)$ of the discontinuous function $\nu(t)$ is of the form

$$\nu_j(t) = -\lambda_j(t)\ \text{sign}\ (\hat{y}_j(t) - y_j(t)), \quad j = 1, \ldots, p, \tag{15}$$

where $\hat{y}_j(t)$ and $y_j(t)$ are the j^{th} entry of the observer output $\hat{y}(t)$ and the plant output $y(t)$, respectively. Each gain $\lambda_j(t)$ of the vector $\lambda(t) \in \mathbb{R}^p$ is governed by

$$\dot{\lambda}_j(t) = \bar{\lambda}_j\ |\hat{y}_j(t) - y_j(t)|, \tag{16}$$

with $\lambda_j(0) > 0$ and $\bar{\lambda}_j > 0$ for $j = 1, \ldots, p$.

Defining the observation errors as $e_1(t) = \hat{z}_1(t) - z_1(t)$ and $e_y(t) = \hat{y}(t) - y(t)$, the error dynamic with respect to

Equations 13 and 14 is then governed by

$$\begin{aligned}\dot{e}_1(t) &= (A_1(\theta) + LA_3(\theta))\, e_1(t),\\ \dot{e}_y(t) &= C_2(\theta)A_3(\theta)e_1(t) + \dot{C}_2(\dot{\theta})C_2^{-1}(\theta)e_y(t)\\ &\quad + C_2(\theta)\left((A_4(\theta) - A_3(\theta)L)\, C_2^{-1}(\theta) - K\right) e_y(t)\\ &\quad - C_2(\theta)E_2 w(t) - C_2(\theta)H_2 f_a(t) + \nu(t).\end{aligned} \tag{17}$$

where $\dot{C}_2(\dot{\theta}) = \frac{\mathrm{d}C_2(\theta)}{\mathrm{d}t}$. As in Equation 2, the matrix $C_2(\theta)$ can be written as $C_2(\theta) = C_{20} + \sum_{i=1}^{m} \theta_i C_{2i}$. Consequently, $\dot{C}_2(\dot{\theta})$ is also affinely dependent on $\dot{\theta} \in \mathbb{R}^m$ as follows

$$\dot{C}_2(\dot{\theta}) = \sum_{i=1}^{m} \dot{\theta}_i C_{2i}. \tag{18}$$

Moreover, based on the assumption that $\dot{\theta}(t) \in P_{\dot{\theta}} := \mathrm{Co}\{\dot{\theta}_{\mathrm{v}_1}, \dot{\theta}_{\mathrm{v}_2}, \dots, \dot{\theta}_{\mathrm{v}_M}\}$, a polytopic representation for $\dot{C}_2(\dot{\theta})$ can be written as $\dot{C}_2(\dot{\theta}) = \sum_{l=1}^{M} \beta_l \dot{C}_2\left(\dot{\theta}_{\mathrm{v}_l}\right)$.

3.1 | Stability of the adaptive sliding mode observer

The transformation T in Equation 11 allows to prove the stability of $e_1(t)$ by selecting an appropriate gain L as in Equation 12, since the boundedness of $e_1(t), t \geqslant 0$, is required for the stability of $e_y(t)$ and the reconstruction of $f_a(t)$ as explained afterwards. The objective is to determine the discontinuous function $\nu(t)$ in Equations 15 such that the system reaches the sliding surface $e_y(t) = 0$ and maintains a sliding motion around the surface.

Theorem 1. The sliding mode of the output observation error $e_y(t)$ in Equation 17, controlled by a discontinuous signal $\nu(t)$ governed by Equations 15 and 16 is established around $e_y(t) = 0$ by selecting $\bar{\lambda}_j > 0$, $\varepsilon_j > 0$ *for* $j = 1, \dots, p$ and obtaining the observer gain matrix K and the matrix L of the form (Equation 12) from the following linear matrix inequality (LMI) conditions evaluated at each vertix $(\theta_{\mathrm{v}_i}, \dot{\theta}_{\mathrm{v}_l})$ for $i, l = 1, \dots, M$:

$$A_1\left(\theta_{\mathrm{v}_i}\right) + LA_3\left(\theta_{\mathrm{v}_i}\right) < 0, \tag{19}$$

$$\begin{aligned}&C_2\left(\theta_{\mathrm{v}_i}\right)\left(\left(A_4\left(\theta_{\mathrm{v}_i}\right) - A_3\left(\theta_{\mathrm{v}_i}\right)L\right) C_2^{-1}\left(\theta_{\mathrm{v}_i}\right) - K\right)\\ &+ \left(\left(A_4\left(\theta_{\mathrm{v}_i}\right) - A_3\left(\theta_{\mathrm{v}_i}\right)L\right) C_2^{-1}\left(\theta_{\mathrm{v}_i}\right) - K\right)^{\top} C_2^{\top}\left(\theta_{\mathrm{v}_i}\right)\\ &+ \dot{C}_2\left(\dot{\theta}_{\mathrm{v}_l}\right) C_2^{-1}\left(\theta_{\mathrm{v}_i}\right) + C_2^{-1^{\top}}\left(\theta_{\mathrm{v}_i}\right) \dot{C}_2^{\top}\left(\dot{\theta}_{\mathrm{v}_l}\right) < 0.\end{aligned} \tag{20}$$

Proof. Let us introduce the following Lyapunov candidate function:

$$V_y\left(e_y(t), \tilde{\lambda}(t)\right) = \frac{1}{2} e_y^{\top}(t) e_y(t) + \frac{1}{2} \tilde{\lambda}^{\top}(t) \Gamma^{-1} \tilde{\lambda}(t), \tag{21}$$

with $\Gamma = \mathrm{diag}(\bar{\lambda}_j)$, $\tilde{\lambda}(t) = \lambda(t) - \lambda^*$, and the vector λ^* to be determined. The derivative of $V_y(t)$ along the error trajectory (Equation 17) is

$$\begin{aligned}\dot{V}_y\left(e_y(t), \tilde{\lambda}(t)\right) &= \frac{1}{2} e_y^{\top}(t)\Big[C_2(\theta)\left((A_4(\theta) - A_3(\theta)L)\, C_2^{-1}(\theta) - K\right) + \left((A_4(\theta) - A_3(\theta)L)\, C_2^{-1}(\theta) - K\right)^{\top} C_2^{\top}(\theta)\Big] e_y(t)\\ &\quad + \frac{1}{2} e_y^{\top}(t)\left(\dot{C}_2(\dot{\theta})C_2^{-1}(\theta) + C_2^{-1^{\top}}(\theta)\dot{C}_2^{\top}(\dot{\theta})\right) e_y(t)\\ &\quad + e_y^{\top}(t)\left[C_2(\theta)A_3(\theta)e_1(t) - C_2(\theta)E_2 w(t) - C_2(\theta)H_2 f_a(t)\right] + e_y^{\top}(t)\nu(t) + \dot{\lambda}^{\top}(t)\Gamma^{-1}\tilde{\lambda}(t).\end{aligned}$$

By defining

$$\begin{aligned}\xi(\theta, \dot{\theta}) &= C_2(\theta)\left((A_4(\theta) - A_3(\theta)L)\, C_2^{-1}(\theta) - K\right)\\ &\quad + \left((A_4(\theta) - A_3(\theta)L)\, C_2^{-1}(\theta) - K\right)^{\top} C_2^{\top}(\theta)\\ &\quad + \dot{C}_2(\dot{\theta})C_2^{-1}(\theta) + C_2^{-1^{\top}}(\theta)\dot{C}_2^{\top}(\dot{\theta}),\end{aligned} \tag{22}$$

the condition $\frac{1}{2} e_y^{\top}(t)\xi(\theta, \dot{\theta})e_y(t) < 0$ holds if the LMI (Equation 20) is satisfied at all the vertices of θ and $\dot{\theta}$.

Furthermore, after assuming that $C_2(\theta)$ is bounded over the trajectories of θ and that $e_1(t)$ is stable, and hence, bounded through LMI (Equation 19), it follows that

$$\begin{aligned}\dot{V}_y\left(e_y(t), \tilde{\lambda}(t)\right) \leqslant \underbrace{\frac{1}{2} e_y^{\top}(t)\xi(\theta, \dot{\theta})e_y(t)}_{<0} + |e_y(t)|^{\top} \underbrace{\left|C_2(\theta)A_3(\theta)e_1(t) - C_2(\theta)E_2 w(t) - C_2(\theta)H_2 f_a(t)\right|_{\max}}_{\Psi_{\max}}\\ - |e_y(t)|^{\top}\lambda(t) + |e_y(t)|^{\top}\tilde{\lambda}(t),\end{aligned} \tag{23}$$

and hence,

$$\dot{V}_y\left(e_y(t), \tilde{\lambda}(t)\right) \leqslant \frac{1}{2} e_y^{\top}(t)\xi(\theta, \dot{\theta})e_y(t) + |e_y(t)|^{\top}\left(\Psi_{\max} - \lambda^*\right). \tag{24}$$

The constant vector λ^* can be selected such that $\gamma = \lambda^* - \Psi_{\max}$ is a positive vector, and hence,

$$\begin{aligned}\dot{V}_y\left(e_y(t), \tilde{\lambda}(t)\right) &\leqslant \frac{1}{2} e_y^{\top}(t)\xi(\theta, \dot{\theta})e_y(t) - |e_y(t)|^{\top}\gamma\\ &\leqslant -|e_y(t)|^{\top}\gamma \leqslant 0.\end{aligned} \tag{25}$$

Consequently, $e_y(t)$ and $\tilde{\lambda}(t)$ are bounded.

Moreover, by integrating Equation 25, it follows that

$$\begin{aligned}\lim_{t\to\infty} \int_0^t |e_y(\tau)|^{\top}\gamma \, \mathrm{d}\tau &\leqslant V_y\left(e_y(0), \tilde{\lambda}(0)\right)\\ &\quad - \lim_{t\to\infty} V_y\left(e_y(t), \tilde{\lambda}(t)\right) \leqslant \infty,\end{aligned} \tag{26}$$

since $V_y\left(e_y(t), \tilde{\lambda}(t)\right)$ is bounded. Therefore, $\lim_{t\to\infty} \int_0^t |e_y(\tau)|^\top \gamma \, d\tau$ is bounded, and it follows that $\gamma^\top |e_y(t)|$ is uniformly continuous in t since $\dot{e}_y(t)$ is bounded. Thus, applying *Barbalat Lemma* results that $\lim_{t\to\infty} \gamma^\top |e_y(t)| = 0$, which leads to $\lim_{t\to\infty} |e_y(t)| = 0$ since γ is a positive vector.

As a result, the convergence of the LPV adaptive sliding mode observer (Equation 14) is demonstrated, as well as the maintenance of the sliding motion around $e_y(t) = 0$, which completes the proof. □

3.2 | Reconstruction of the actuator fault

After the sliding motion is maintained, the actuator fault signal $f_a(t)$ can be reconstructed from the output error based on the principle of equivalent control.[22,26] The equivalent control $\nu_{\text{eq}}(t)$ represents the average behavior of $\nu(t)$ that is the effort necessary to maintain the motion on the sliding surface $\hat{y}(t) - y(t) = 0$. If the induced chattering by the proposed observer is significant, the equivalent control $\nu_{\text{eq}}(t)$ can be obtained from filtering the discontinuous input $\nu(t)$ in Equation 15 that only depends on the measurable outputs $y(t)$ of the LPV model and the observer outputs $\hat{y}(t)$. However, $\nu(t)$ is also affected by the presence of the model uncertainties and disturbances $w(t)$ as well as the faults. After reaching and maintaining the sliding motion, the error dynamics can be written as $e_y(t) = 0$ and $\dot{e}_y(t) = 0$, and with $e_1(t) = 0$, Equations 17 will lead to

$$0 = -C_2(\theta)E_2 w(t) - C_2(\theta)H_2 f_a(t) + \nu_{\text{eq}}(t). \tag{27}$$

With $C_2(\theta)$ being nonsingular and the structure of E_2 and H_2 as in Equation 5, we obtain

$$0 = -E_{22} w(t) - H_{22} f_a(t) + \left(C_2^{-1}(\theta)\nu_{\text{eq}}(t)\right)_{\tilde{q}}, \tag{28}$$

where $\left(C_2^{-1}(\theta)\nu_{\text{eq}}(t)\right)_{\tilde{q}}$ is the last $\tilde{q}$ components of $C_2^{-1}(\theta)\nu_{\text{eq}}(t)$. Furthermore, to separate the effects of the uncertainty $w(t)$ on the actuator fault reconstruction as in the work of Yan and Edwards,[25] we consider a matrix $W \in \mathbb{R}^{\tilde{q}\times\tilde{q}}$ such that

$$W[E_{22}\ H_{22}] = \begin{bmatrix} M_1 & 0 \\ 0 & M_2 \end{bmatrix}. \tag{29}$$

This equality can be satisfied under the condition: $\text{Im}(E_{22}) \cap \text{Im}(H_{22}) = 0$, where $\text{Im}(\cdot)$ denotes the image of a matrix. Therefore, using Equation 29, it follows that

$$\begin{bmatrix} M_1 w(t) \\ M_2 f_a(t) \end{bmatrix} = W\left(C_2^{-1}(\theta)\nu_{\text{eq}}(t)\right)_{\tilde{q}}. \tag{30}$$

If W_q is considered as the vector composed of the last q rows of W, one can obtain

$$W_q\left(C_2^{-1}(\theta)\nu_{\text{eq}}(t)\right)_{\tilde{q}} = M_2 f_a(t), \tag{31}$$

and finally, the actuator fault severity estimate is reconstructed as

$$\hat{f}_a(t) = M_2^{-1} W_q\left(C_2^{-1}(\theta)\nu_{\text{eq}}(t)\right)_{\tilde{q}}. \tag{32}$$

Remark 1. As discussed in previous studies,[22,26,27] 1 way to recover the equivalent output injection signal is by using a low-pass filter. Another alternative approach is to approximate the discontinuous function $\nu(t)$ by a continuous one as follows

$$\nu_j(t) = -\lambda_j(t)\, \frac{\hat{y}_j(t) - y_j(t)}{|\hat{y}_j(t) - y_j(t)| + \delta}, \quad j = 1, \ldots, p, \tag{33}$$

where δ is a small scalar. The new equivalent output injection in Equation 33 can be approximated to any degree of accuracy for a small enough choice of δ. This method is normally used when a first-order sliding mode observer is designed. This type of observer induces a high chattering of the estimated signals around their corresponding real values, and hence, a filtering technique will have to be used, like in 2 previous studies.[25,27] In the proposed adaptive sliding mode observer, the chattering is significantly reduced because of the observer gain is adaptively increased to reach the required value to overcome the faults and uncertainties. Therefore, the implementation of the new equivalent injection is not needed for fault reconstruction.

4 | APPLICATION EXAMPLES

To illustrate the effectiveness of the LPV adaptive sliding mode observer (Equation 14), two LPV models are considered: the first LPV model has a fixed distribution matrix, which allows a comparison of the adaptive sliding mode to a first-order sliding mode observer, and the second LPV model has a time-varying output distribution matrix.

4.1 | Model with fixed *C*matrix

Let us consider a single-link flexible joint robotic manipulator, where the system nonlinearities are due to the joint flexibility modeled as a stiffened torsional spring and the gravitational force. The dynamic model given in the work of Fan and Arcak[28] is as follows

$$\begin{aligned}
\dot{\psi}_1(t) &= \omega_1(t), \\
\dot{\omega}_1(t) &= \frac{1}{J_1}\left(k_1(\psi_2(t) - \psi_1(t)) + k_2(\psi_2(t) - \psi_1(t))^3\right) \\
&\quad - \frac{B_{\text{v}}}{J_1}\omega_1(t) + \frac{K_\tau}{J_1}u(t), \\
\dot{\psi}_2(t) &= \omega_2(t), \\
\dot{\omega}_2(t) &= -\frac{1}{J_2}\left(k_1(\psi_2(t) - \psi_1(t)) + k_2(\psi_2(t) - \psi_1(t))^3\right) \\
&\quad - \frac{m_{\text{l}} g h}{J_2}\sin\psi_2(t) \\
&\quad + \Psi(\psi_1(t), \omega_1(t), \psi_2(t), \omega_2(t), t),
\end{aligned} \tag{34}$$

where ψ_1 and ω_1 are the motor position and velocity, respectively; ψ_2 and ω_2 are the link position and velocity, respectively; J_1 is the inertia of the DC motor, J_2 is the inertia of the link, $2h$ is the length of the link and m_{l} represents its mass, B_{v}

is the viscous friction, k_1 and k_2 both are positive constants, and K_τ is the amplifier gain. It is assumed that the motor position, motor velocity, and the sum of link velocity and link position are measurable. The quantity $\Psi(\psi_1, \omega_1, \psi_2, \omega_2, t)$ satisfying $|\Psi(\cdot)| \leqslant |\omega_1 \sin\omega_2| \exp(-t)$ represents the uncertainty affecting the system.

After grouping all the nonlinear terms of Equation 34 in the scheduling vector $\theta(t) = [\theta_1(t), \theta_2(t), \theta_3(t)]^\top$ such that

$$\begin{aligned} \theta_1(t) &= \psi_1^2(t) + 2\psi_2(t), \\ \theta_2(t) &= \psi_2^2(t), \\ \theta_3(t) &= \frac{\sin\psi_2(t)}{\psi_2(t)}, \end{aligned} \tag{35}$$

the matrices of the LPV model representation (Equation 1) are written as

$$\begin{aligned} A(\theta) &= \begin{bmatrix} 0 & 1 & 0 & 0 \\ -\frac{k_1}{J_1} - \frac{k_2}{J_1}\theta_1 & -\frac{B_v}{J_1} & \frac{k_1}{J_1} + \frac{k_2}{J_1}\theta_2 & 0 \\ 0 & 0 & 0 & 1 \\ \frac{k_1}{J_2} + \frac{k_2}{J_2}\theta_1 & 0 & -\frac{k_1}{J_2} - \frac{k_2}{J_2}\theta_2 - \frac{m_1 g h}{J_2}\theta_3 & 0 \end{bmatrix}, \\ B &= \begin{bmatrix} 0 \\ \frac{K_\tau}{J_1} \\ 0 \\ 0 \end{bmatrix}, C = \begin{bmatrix} 1 & 0 & 0 & 0 \\ 0 & 1 & 0 & 0 \\ 0 & 0 & 1 & 1 \end{bmatrix}, \\ E &= \begin{bmatrix} 0 & 0 & 0 & 1 \end{bmatrix}^\top, \text{ and } H = B. \end{aligned} \tag{36}$$

According to Lemma 1, to obtain the LPV model (Equation 36) of the form (Equation 10), a change of coordinate is done with the matrix $\mathcal{T} = \begin{bmatrix} 0 & 0 & 1 & 0 \\ 1 & 0 & 0 & 0 \\ 0 & -1 & 0 & 0 \\ 0 & 0 & -1 & -1 \end{bmatrix}$ and the resulting matices will be obtained as

$$\begin{aligned} A_1 &= -1,\ B_2 = H_2 = \begin{bmatrix} 0 \\ -\frac{K_\tau}{J_1} \\ 0 \end{bmatrix},\ E_2 = \begin{bmatrix} 0 \\ 0 \\ -1 \end{bmatrix}, \\ C_2 &= \begin{bmatrix} 1 & 0 & 0 \\ 0 & -1 & 0 \\ 0 & 0 & -1 \end{bmatrix}. \end{aligned} \tag{37}$$

At this point, the transformation T in Equation 11 is not necessary since $e_1(t)$ is stable because of that $A_1 < 0$. Therefore, $L = [000]$ and $T = \mathbb{I}_{3\times3}$. By solving the LMI (Equation 20) for the 8 vertices of θ, the observer gain is obtained as $K = 10^3 \begin{bmatrix} 4.667 & -0.0343 & 0.0114 \\ 0.0135 & -4.6880 & 0.3218 \\ -0.0081 & -0.2938 & -4.6739 \end{bmatrix}$. Then, since $\mathrm{Im}(E_{22}) \cap \mathrm{Im}(H_{22}) = 0$, a suitable choice of the decoupling matrix is $W = \begin{bmatrix} 0 & 1 \\ 1 & 0 \end{bmatrix}$. Finally, the reconstruction of any fault f is obtained from Equation 32.

For the control design purpose, a linear state feedback $u(t) = \begin{bmatrix} -16.2 & -12.1 & -39.7 & -25.6 \end{bmatrix} x(t)$is used to stabilize the system. The actuator fault starting with a ramp, then becoming sinusoidal is considered for this example.

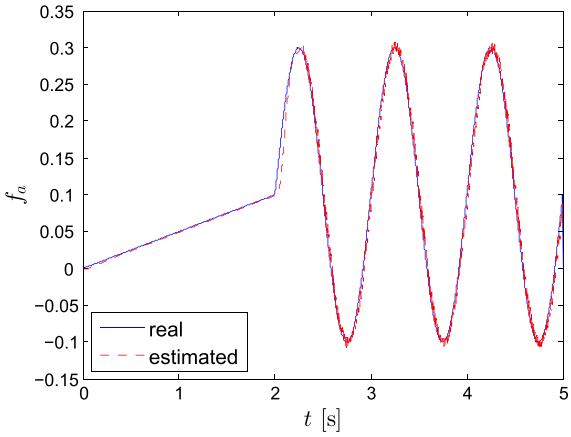

FIGURE 1 Fault reconstruction with the proposed linear parameter–varying adaptive Sliding Mode Observer (SMO) [Colour figure can be viewed at wileyonlinelibrary.com]

As observed from Figure 1, the fault is very well reconstructed with the LPV adaptive sliding mode observer (Equation 14). The presence of the fault is instantaneously detected, and the fault is estimated with a mean square percentage error of 0.086% of the real fault signal. Moreover, it should be noted that there is no need to use a low-pass filter for the proposed adaptive observer in this example since the adaptive observer gain was sufficient to guarantee the stability of the error without any over estimation, and hence, no chattering is induced for the fault estimation.

To emphasize on the advantages of the adaptive approach, we design a first-order LPV sliding mode[17] for the transformed LPV model (Equation 13) with the discontinuous function

$$\nu_j(t) = -\lambda_j \,\mathrm{sign}\,(\hat{y}_j(t) - y_j(t)), \tag{38}$$

considered with λ constant instead of being time-varying as in Equations 15 and 16. The constant observer gain λ must satisfy $\lambda > \Psi_{\max}$ to ensure the negativity of $\dot{V}_y$ in Equation 23. The fault signal reconstructed with a first-order LPV sliding mode observer, as shown in Figure 2, is filtered by a low-pass filter of time constant equal to 0.01 seconds because of high chattering encountered by the estimation around the fault real shape. The mean square percentage error of the filtered estimation is 0.0758% of the real fault. Both errors are very small, which emphasizes the efficiency of the sliding mode technique. The adaptive observer remains advantageous since it does not require any bounds on the uncertainty or the fault and also due to its ability to reduce the inevitable chattering phenomenon. Moreover, it should be emphasized that $\Psi_{\max}$ depends on the bound of the error signal $e_1(t)$ that is not priori available. Therefore, 1 should select a very high-conservative observer gain λ to satisfy $\lambda > \Psi_{\max}$ that as mentioned above will lead to high chattering in fixed sliding mode observer approaches.

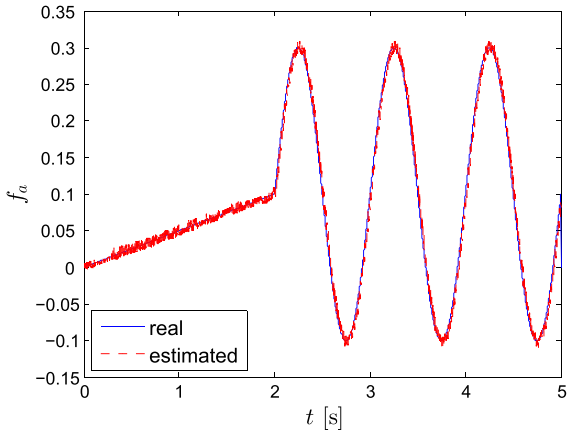

FIGURE 2 Fault reconstruction with a first-order linear parameter–varying SMO with a constant gain [Colour figure can be viewed at wileyonlinelibrary.com]

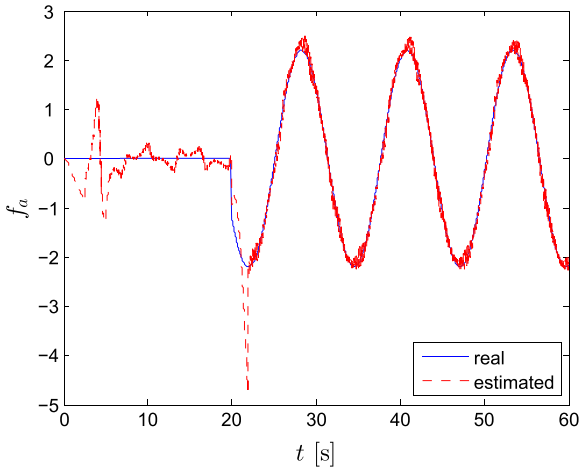

FIGURE 3 Fault reconstruction for the second example [Colour figure can be viewed at wileyonlinelibrary.com]

4.2 | Model with time-varying $C(\theta)$

Let us consider a numerical LPV model with time-varying distribution matrix. The matrices are as follows:

$$A(\theta) = \begin{bmatrix} 0.1\theta_2 & -1+0.2\theta_2 & 0.015\theta_3 \\ 1+0.3\theta_1+0.1\theta_2 & -0.5+0.2\theta_2 & 0 \\ -0.019+0.015\theta_3 & 0.977-0.015\theta_3 & -0.1 \end{bmatrix},$$
$$C(\theta) = \begin{bmatrix} -1+\theta_2 & 1 & 0 \\ 0 & 1 & 0 \end{bmatrix},$$
$$E = \begin{bmatrix} -2 \\ 1 \\ 0.01 \end{bmatrix} \text{ and } H = \begin{bmatrix} 1 \\ 0.02 \\ 0 \end{bmatrix}, \tag{39}$$

where the scheduling variables are sinusoidal waves as

$$\begin{aligned} \theta_1(t) &= 2\sin(0.5t), \\ \theta_2(t) &= 0.5\sin(2t), \\ \theta_3(t) &= 0.5+0.5\sin(0.5t). \end{aligned} \tag{40}$$

The above system is also under sinusoidal disturbance and actuator fault of magnitudes equal to 0.3 and 2.2, respectively, and angular frequencies equal to 1 rad/s and 0.5 rad/s starting from 20 seconds, respectively. After a change of coordinate with the matrix $\mathcal{T} = \begin{bmatrix} 0 & 0 & 0.001 \\ -1 & 1 & 0 \\ 0 & 1 & 0 \end{bmatrix}$, according to Lemma 1, the LPV model will be of the form (Equation 10) with

$$E_{22} = \begin{bmatrix} 3 \\ 1 \end{bmatrix}, H_{22} = \begin{bmatrix} -0.98 \\ 0.02 \end{bmatrix}, \; C_2(\theta) = \begin{bmatrix} 1-\theta_2 & \theta_2 \\ 0 & 1 \end{bmatrix}. \tag{41}$$

A stable observer is designed by solving the LMI (Equation 20) for 16 vertices determined from the bounds of θ and $\dot{\theta}_2$, which results in $K = \begin{bmatrix} -1.2857 & 0.05 \\ 0.5 & 0.947 \end{bmatrix}$. Then, the actuator fault can be directly reconstructed by Equation 32 after decoupling the fault from the disturbance with the matrix $W = \begin{bmatrix} 1 & 49 \\ 1 & -3 \end{bmatrix}$.

After analyzing Figure 3, the LPV adaptive sliding mode observer (Equation 14) shows its ability to rapidly detect (in 0.01 s) the presence of the fault and to ideally follow the fault profile after 2 seconds from its appearance. The mean square percentage error is calculated to be 0.4% of the real fault. It should be noted that in this simulation, there is also no need to use a low-pass filter for the discontinuous function $v(t)$.

5 | CONCLUSIONS

In this paper, an LPV adaptive sliding mode observer is developed for actuator fault detection, isolation, and reconstruction in a class of LPV systems. By means of its adaptive gain, the proposed observer is able to cope with time-varying output distribution matrix in the LPV systems by only assuming a nonsingular distribution matrix with bounded derivative. The LPV sliding mode observer, examined with fixed and time-varying distribution matrices for LPV systems, is validated with Matlab/Simulink. Compared with a first-order LPV sliding mode designed for an application example, the proposed adaptive LPV observer reveals a desired performance in both simultaneous detection and fast tracking of the fault profiles without the need for any filtering technique or a priori knowledge of the fault upper bound.

ACKNOWLEDGMENTS

This publication was made possible by NPRP grant 5-574-2-233 from the Qatar National Research Fund (a member of Qatar Foundation). The statements made herein are solely the responsibility of the authors.

REFERENCES

1. Mohammadpour J, Scherer C. *Control of Linear Parameter Varying Systems with Applications*. Springer-Verlag: New York, Dordrecht, Heidelberg, London, 2012.

2. Rugh WJ, Shamma JS. Research on gain scheduling. *Automatica* 2000; 36:1401–1425.
3. Tóth R. *Modeling and Identification of Linear Parameter-Varying Systems*. Springer–Verlag: Berlin, Heidelberg, 2010.
4. Tóth R, Van de Wal M, Heuberger P, Van den Hof P. LPV identification of high performance positioning devices. *Proceedings of the American Control Conference*, San Francisco, CA, USA, 2011;151–158.
5. Abbas HS, Ali A, Hashemi SM, Werner H. LPV state-feedback control of a control moment gyroscope. *Control Eng Pract* 2014; 24(3):129–137.
6. Bachnas A, Tóth R, Ludlage J, Mesbah A. A review on data-driven linear parameter-varying modeling approaches: a high-purity distillation column case study. *J Process Control* 2014; 24(4):272–285.
7. Abdalla MO, Nobrega EG, Grigoriadis KM. Fault detection and isolation filter design for linear parameter varying systems. *Proceedings of the American Control Conference*, IEEE, Arlington, VA, USA; 2001;3890–3895.
8. Bokor J, Balas GJ, Detection filter design within the LPV framework. In *Proceedings of the* 19th *Digital Avionics Systems Conference, DASC*, Philadelphia, PA, USA, vol. 2 IEEE, 2000;6A3–1.
9. Kulcsár B, Verhaegen M. Robust inversion based fault estimation for discrete-time LPV systems. *IEEE Trans Autom Control* 2012; 57(6):1581–1586.
10. Shi F, Patton RJ. A robust LPV fault detection approach using parametric eigenstructure assignment. *Ukacc International Conference on Control (CONTROL)*, IEEE, Cardiff, United Kingdom 2012;467–472.
11. Chen L, Patton RJ. Polytope LPV estimation for non-linear flight control. *The Proc IFAC World Congress* 2011:6680–6685.
12. Grenaille S, Henry D, Zolghadri A. A method for designing fault diagnosis filters for LPV polytopic systems. *J Control Sci Eng* 2008; 2008:1.
13. Salar A, Meskin N, Khorasani K. A novel affine qLPV model derivation method for fault diagnosis h-∞ performance improvement. *2015 American Control Conference (ACC)*, Chicago, IL, USA; July 2015;823–830.
14. Efimov D, Raissi T, Zolghadri A. Set adaptive observers for LPV systems: application to fault detection. *ASME J Dyn Syst Meas Control* December 2013; vol 136; https://hal.archives-ouvertes.fr/hal-01126274.
15. Kovács L, Kulcsár B, Bokor J, Benyo Z. LPV fault detection of glucose-insulin system. 14th *Mediterranean Conference on Control and Automation, MED '06*, Ancona, Italy; June 2006;1–5.
16. Alwi H, Edwards C. Development and application of sliding mode LPV fault reconstruction schemes for the ADDSAFE benchmark. *Control Eng Pract* 2014; 31:148–170.
17. Alwi H, Edwards C. Robust fault reconstruction for linear parameter varying systems using sliding mode observers. *Int J Robust Nonlinear Control* 2014; 24(14):1947–1968.
18. Huang Y-J, Kuo T-C, Chang S-H. Adaptive sliding-mode control for nonlinear systems with uncertain parameters. *Syst Man Cybern Part B: Cybern IEEE Trans on* 2008; 38(2):534–539.
19. Plestan F, Shtessel Y, Bregeault V, Poznyak A. New methodologies for adaptive sliding mode control. *Int J Control* 2010; 83(9):1907–1919.
20. Rahme S, Meskin N. Adaptive sliding mode observer for sensor fault diagnosis of an industrial gas turbine. *Control Eng Pract* 2015; 38:57–74.
21. Menon PP, Edwards C, Shtessel YB. Adaptive sliding mode observation in a network of dynamical systems. *Int J Adapt Control Signal Process* 2016; 30:1465–1477.
22. Utkin V*Sliding Modes in Control and Optimization*. Springer-Verlag: Berlin, Germany, 1992.
23. Mercorelli P. An antisaturating adaptive preaction and a slide surface to achieve soft landing control for electromagnetic actuators. *IEEE/ASME Trans Mechatron* 2012; 17(1):76–85.
24. Dey S, Mohon S, Pisu P, Ayalew B. Sensor fault detection, isolation, and estimation in lithium-ion batteries. *IEEE Trans Control Syst Technol* 2016; 24(6):2141–2149.
25. Yan X-G, Edwards C. Nonlinear robust fault reconstruction and estimation using a sliding mode observer. *Automatica* 2007; 43(9):1605–1614.
26. Floquet T, Edwards C, Spurgeon S. On sliding mode observers for systems with unknown inputs. *Int J Adapt Control Signal Process* 2007; 21(8-9):638–656.
27. Edwards C, Spurgeon S, Patton R. Sliding mode observers for fault detection and isolation. *Automatica* 2000; 36:541–553.
28. Fan X, Arcak M. Observer design for systems with multivariable monotone nonlinearities. *Syst Control Lett* 2003; 50(4):319–330.

How to cite this article: Rahme S, Meskin N, Mohammadpour J. Adaptive sliding mode-based diagnosis of actuator faults for LPV systems. *Int J Adapt Control Signal Process*. 2017. doi:10.1002/acs.2761